Available online at www.sciencedirect.com
ScienceDirect
Advances in Space Research xxx (2008) xxx–xxx
ADVANCES IN SPACE RESEARCH (a COSPAR publication)
www.elsevier.com/locate/asr

Exploring the global shock scenario at multiple points between sun and earth: The solar transients launched on January 1 and September 23, 1978

D.B. Berdichevsky [a,*], D.V. Reames [a], C.-C. Wu [b], R. Schwenn [c], R.P. Lepping [a], R.J. MacDowall [a], C.J. Farrugia [d], J.-L. Bougeret [e], C. Ng [a], A.J. Lazarus [f]

[a] NASA/GSFC, Greenbelt, MD 20771, USA
[b] University Alabama, Huntsville, AL 35899, USA
[c] Max-Planck-Institut für Aeronomie, D 37191 Katlenburg-Lindau, Germany
[d] University New Hampshire, Durham, NH 03824, USA
[e] Observatoire de Paris, Meudon, France
[f] MIT Space Science, Cambridge, MA 02139, USA

Received 27 October 2004; received in revised form 5 March 2008; accepted 13 March 2008

Abstract

We revisit the transient interplanetary events of January 1 and September 23, 1978. Using in-situ and remote sensing observations at locations widely separated in longitudes and distances from the Sun, we infer that in both cases the overall shock surface had a very fast "nose" region with speeds >900 and >1500 km^{-1} in the January and September events, respectively, and much slower flank speeds (~600 km^{-1} or less), suggesting a shock surface with a strong speed gradient with heliospheric longitude. The shock-nose regions are thus likely efficient acceleration sites of MeV ions, even at 1 AU from the Sun. Our 3D magnetohydrodynamics modeling suggests that a 24° × 24° localized disturbance at 18 solar radii injecting momentum 100 times the background solar wind input over 1 h can produce a disturbance in semi-quantitative agreement with the observed shock arrival time, plasma density and velocity time series in the January 1978 event.
© 2008 Published by Elsevier Ltd on behalf of COSPAR.

Keywords: Gradual SEP events; Collisionless shocks; Shock MHD modeling

1. Introduction

Very fast interplanetary coronal mass ejections (CMEs) ($\geqslant$800 km^{-1}) are known to often be associated with moderate to very intense enhancement in the intensity of particles with kinetic energy in the tens of MeV to the hundreds or thousands of MeV per nucleon range (e.g., Reames, 1999a). However, there is considerable variation in the intensities of these solar energetic particle (SEP) intensities for different observed CMEs having similar observed speeds in the plane of the sky (Reames, 1999b; Kahler, 2001). A high ionization level (>10^4 times a γ ray with the same energy) by penetrating ions makes this radiation source dangerous, even at relatively moderate intensity. And a very high intensity event (like the September 29, 1989 case) would have produced over the 8-h interval of its most intense SEP enhancement flux in Earth's vicinity and behind a shielding of a 5 cm thick Al wall, a dose of more than 5× the United States' annual accepted maximum dose of 15 rem radiation a year for radiation workers at ground level (Reames, 2001; Turner, 2001).

The January and September 1978 events have been studied before using multiple spacecraft observations: The January 1 event for the interplanetary magnetic cloud (IMC) (Burlaga et al., 1981); The September 23 event for the spec-

* Corresponding author. Tel.: +1 303 286 2510; fax: +1 301 286 1433.
E-mail address: dbberdi@yahoo.com (D.B. Berdichevsky).

0273-1177/$34.00 © 2008 Published by Elsevier Ltd on behalf of COSPAR.
doi:10.1016/j.asr.2008.03.026

tral characteristics of the proton fluxes (Reames et al., 1996, 1997). Here we investigate the connection between a moderate and an intense SEP event to global aspects of the transient driven shock in the inner heliosphere out to >1 AU. In Section 2 we present the inter-planetary observations. Section 3 discusses the modeling of the shock. Conclusions are given in Section 4.

2. Interplanetary observations

A moderate SEP (<56 MeV) particle event started at ~21 UT on January 1, 1978 and lasted at least seven days. Observations are from Helios 1, Helios 2, Voyager 1, and Voyager 2 at widely separated heliospheric longitude and distance and from the near Earth spacecraft IMP 8 and ISEE 3 (see Table 1). Fig. 1a shows the proton intensity for channels in the 3–60 MeV range as a function of time for the period January 1–8, 1978 at Helios 1, Helios 2 and IMP-8. On the right, the solar wind speed time series is presented for the corresponding spacecraft (but for ISEE-3 instead of IMP-8) in the same time interval. A 2N flare at E06S21 in McMath region 15081 peaking in intensity at 2145 UT on January 1, 1978 is the solar association with this gradual SEP event, shock and ejecta (Burlaga et al., 1981; Reames et al., 1996).

The differences in p-intensities observed at different longitudes by Helios 1, Helios 2 and IMP-8 (Fig. 1a) suggest that Helios 1 was seeing a western-to-central event with early good connection to the shock nose (see e.g., Heras et al., 1988; Cane et al., 1988; Reames et al., 1996). The other two spacecraft see a rather poorly connected event, suggestive of seeing particles coming from an Eastern shock. The time of that arrival is easier to identify in the solar wind speed time series in Fig. 1b, and indicates that at Helios 1 the passage is 6.2 h earlier than at Helios 2, which was located 2% closer to the Sun than Helios 1. Also the shock speed appears much larger at Helios 1 (Fig. 1b). At Helios 1 after the shock passage there is a decrease in SEP intensity, but this can be followed only for about 90 min, after which there is data gap of ~7 h. This overall higher SEP intensity at Helios 1 before the shock passage tells us we are West of the shock acceleration region, but the large speed discontinuity (top right in Fig. 1) suggests that we may be nearer to the nose portion of the shock surface than at other in-situ locations where its passage is observed. On the other hand, the further enhancement of the SEP intensity at Helios 2 and IMP-8 after the shock passage suggests that the best connection to the stronger shock region (shock nose) occurs after the in-situ shock passage. Also the later nearly one order of magnitude decrease in SEP intensity, marked by inclined dash lines in Fig. 1a and b, is consistent with the passage of the IMC at the different longitude locations (e.g., Richardson et al., 1996). This start time of the hindrance in the SEP intensities also coincides with the beginning of this event invariant SEP spectra (Reames et al., 1997).

A closer look at the shock is needed to substantiate the above interpretations based on the SEP profiles at different locations. The solar wind parameters of shock passage at Helios 1 are presented in Fig. 2. From top to bottom we see the proton density, the solar wind velocity x, y and z directions in the solar ecliptic (SE) coordinate system, the proton temperature, and the magnitude and orientation in SE of the magnetic field in the three bottom panels. Shaded areas show the up (down)-stream regions used in the Rankine–Hugoniot (R–H) analysis of the shock (Berdichevsky et al., 2000, 2001), presented in Table 2. The analysis confirms the interpretation based on SEP intensity about the in-situ encounter at Helios 1 with the Eastern/Central portion of the global shock surface, and with its Western side at ~2 AU at Voyager. On the other hand, the SEP time series show clear indicators that at Earth the event was propagating Eastward. Consequently, at Helios 2, and much closer to Earth, at ISEE-3 and IMP-8, the in-situ shock surface appears to be the *Eastern side of a global* shock surface. The R–H analysis of the Helios 2 data further establishes that the velocity $(-450, 72, 55)\ \mathrm{km}^{-1}$ of the 1450 UT shock on January 3 was slow. It is the much faster moving pressure pulse $(-600, -50, 0)\ \mathrm{km}^{-1}$ at 1633 UT that is consistent with the lateral westward shock surface, and it is the one used in the sketch of the global shock in Fig. 3.

The top panel in Fig. 2 illustrates that at its passage over Helios 1, the shock strongly compressed the plasma in the downstream region. Further, Table 2 shows that the shock at Helios 1 was near the strong shock limit for shock compression. These are shocks known to be capable of accelerating particles at 1 AU. A well-documented example is the

Table 1
Location of spacecraft for the January and September 1978 events

Spacecraft	Event 1			Event 2		
	Date and time	D (AU)	Long.	Date and time	D (AU)	Long.
Helios 1	January 3 0838	0.95	40E	September 25	0.74	120W
Helios 2	January 3 1450	0.93	6E	September 25★†	0.71	160W
IMP-8	January 3 2040	1.0	0	September 25§	1.0	0
ISEE-3	January 3§	0.99	0	September 25§	0.99	0
Voyager 1	January 6★	1.97	22E	October 6	4.4	122W
Voyager 2	January 6 0001	1.95	24E	October 5★	4.0	122W

Indicated in Table 1 are heliospheric distance (D) from the Sun and helio-longitude for the time of the shock at each SC. ★, a few hours plasma and IMF void at shock passage; §, a few hours plasma void at shock passage; †, possibly a different ejecta passage.

Please cite this article in press as: Berdichevsky, D.B. et al., Exploring the global shock scenario at multiple points between sun ..., J. Adv. Space Res. (2008), doi:10.1016/j.asr.2008.03.026

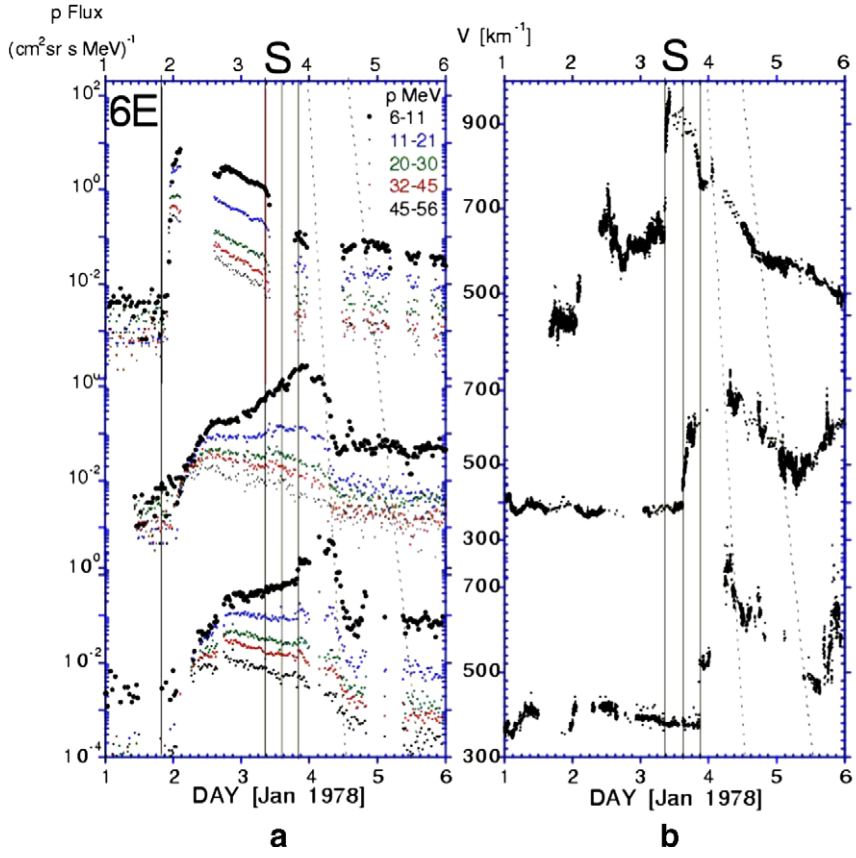

Fig. 1. From top to bottom (a) proton (p) intensities at H1, H2, and IMP-8. Energy channel labels are given on the top-right side. (b) solar wind speed V at H1, H2 and ISEE3.

Earth's bow shock [see e.g., the section "Upstream Waves and Particles" in J. Geophys. Res. 86(A6), 4317–4538, 1981]. The center-point in Fig. 3 indicates the Sun, and the circle is the one astronomical unit (AU) distance from the Sun. The arrows and perpendicular lines, in the sketch in Fig. 3, represents speed and orientation for each shock and the orientation of the shock surface, respectively, at each location where the shock in-situ passage is observed (at Helios 1 (H1), Voyager 2 (V2), Helios 2 (H2) and ISEE-3 (I3).

The September 23–25, 1978 SEP event is intense at all spacecraft within 1 AU (see Fig. 7 in Reames et al., 1996). The solar signatures are a bright optical flare at N35W50, a large, long duration soft X-ray flare, with peak intensity X1, at 0958 UT on September 23, 1978, the onset of type III radio burst, 1003 UT, indicated in Fig. 4, high intensity metric radio burst, and an associated shock with a transit speed to Earth of 910 km^{-1} (Cane, 1985). This is also a major SEP particle event: At all locations within 1 AU the enhancement in the SEP intensity are large, up to 2×10^3 and 1 p/(cm^2 sr s MeV) in 3 and 45 MeV protons, respectively, (Fig. 7 in Reames et al., 1996). However, the spacecraft on the flanks (event 2, Table 1) see at the shock passages lower speeds $\leqslant$600 km^{-1} downstream of the shocks, well below the shock transit speeds. Because the location of the event is 50° West of Earth and apparently East of the other spacecraft locations (see Table 1), we investigate the shock speed of the nose remotely. We use the ISEE-3 radio instrument (Knoll et al., 1978). This event produced extraordinarily well-defined, continuous kilometric type II radiation bursts (Fig. 4), as well as higher frequency emissions (metric signal) nearer to the Sun; the radio emissions covered the whole spectrum and were unusual for their high intensity, from metric or shorter wave length to the kilometric range. The drift of the type II radio emissions in Fig. 4 are interpreted as a very fast moving radio source, here interpreted as the shock remote sensing, that produces radio emissions on DOY 267 (September 24). The arrow to the right in Fig. 4 shows radio emissions compatible with a 1 AU, remote, shock passage nearly 20 h before its in-situ passage at Earth (0718 UT on September 25). The spinning of the spacecraft and the radio instrument antennas produces at each frequency of interest, a modulation that allows for identification of the likely source-location of the radio signal (see e.g., Fainberg, 1979; Fainberg et al., 1985), with the help of a plasma model of the heliosphere.

Fig. 5 shows, in heliographic coordinates, the derived source location of the radio emissions (crosses) at selected frequency values. When we combine the westward location of the radio emission source (the front side region of the shock) in the inner heliosphere, with the time of the emitted

Please cite this article in press as: Berdichevsky, D.B. et al., Exploring the global shock scenario at multiple points between sun ..., J. Adv. Space Res. (2008), doi:10.1016/j.asr.2008.03.026

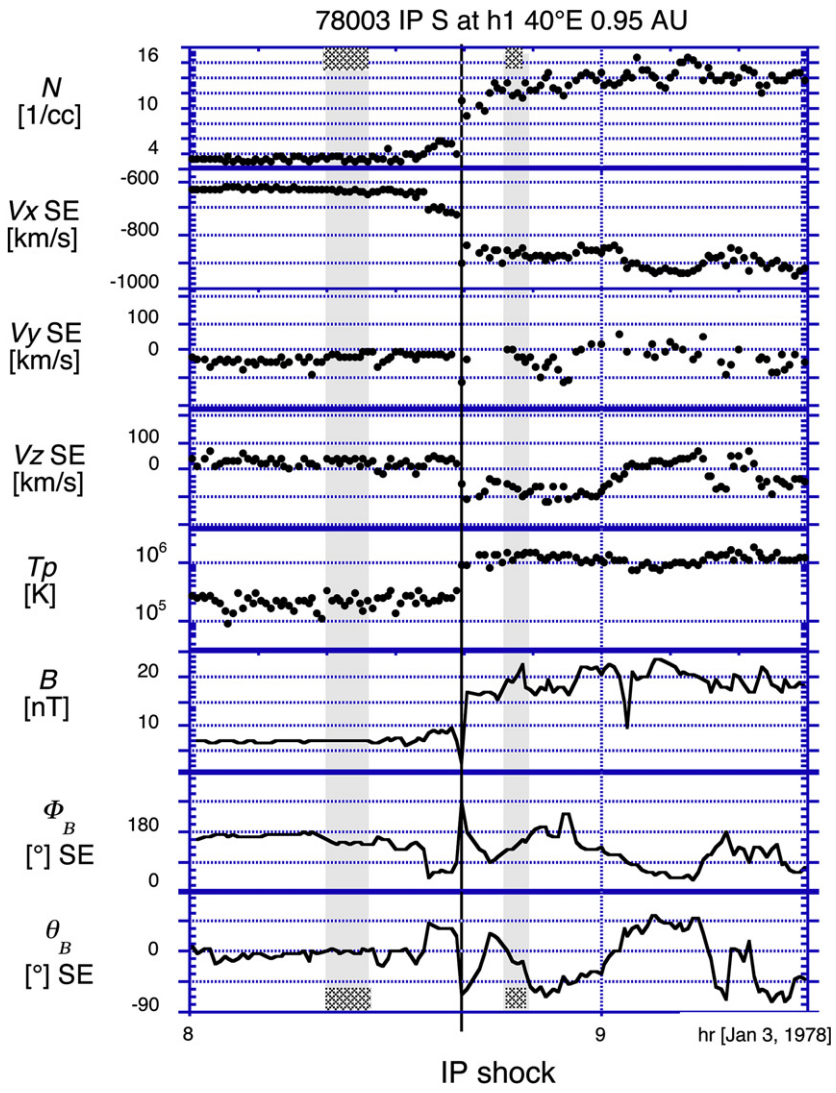

Fig. 2. As a function of time (hour), from top to bottom each panel shows the p number N, SE velocity components Vx, Vy, Vz, p-temperature T, magnetic field B, and its azimuth (ϕ) and latitude (θ) angles at the shock at Helios 1.

Table 2
Event 1 in-situ shock normal $\mathbf{n}_S$, speed V_S (observer frame), and compression

Spacecraft time	$\mathbf{n}_S$ (SE coordinates)	V_S (km^{-1})	Ndw/Nup	Bdw/Bup
Helios 1 Jan 3 0838	−0.955, 0.10, −0.28	950	3.7–4.0	3.2 ± 0.8
Voyger 2 Jan 6 0001	−0.80, −0.32, 0.50	600	3.2–3.6	3.2 ± 0.3

The transit velocity at Helios 1 (Voyager 2) is 1130 (824) km^{-1}.

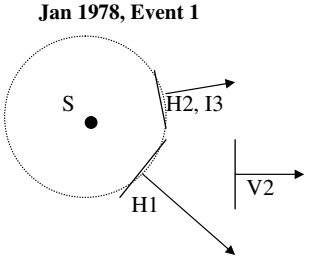

Fig. 3. Sketch of shock directions and shock planes at three in-situ shock passages.

radio signal in Fig. 4, we infer the presence of a nose region of the shock that is moving very fast ($\geqslant$1600 km^{-1}), even at 1 AU.

3. The 3D MHD modeling of the Jan 1–7, 1978 event

We compare in Fig. 6 the solar wind time-of-arrival at two spacecraft with the Han–Detman (Han et al., 1988; Detman et al., 1991; Wu et al., 2005) 3D MHD model prediction for two different initial model conditions. The transient start location is modeled by a perturbation in

Please cite this article in press as: Berdichevsky, D.B. et al., Exploring the global shock scenario at multiple points between sun ..., J. Adv. Space Res. (2008), doi:10.1016/j.asr.2008.03.026

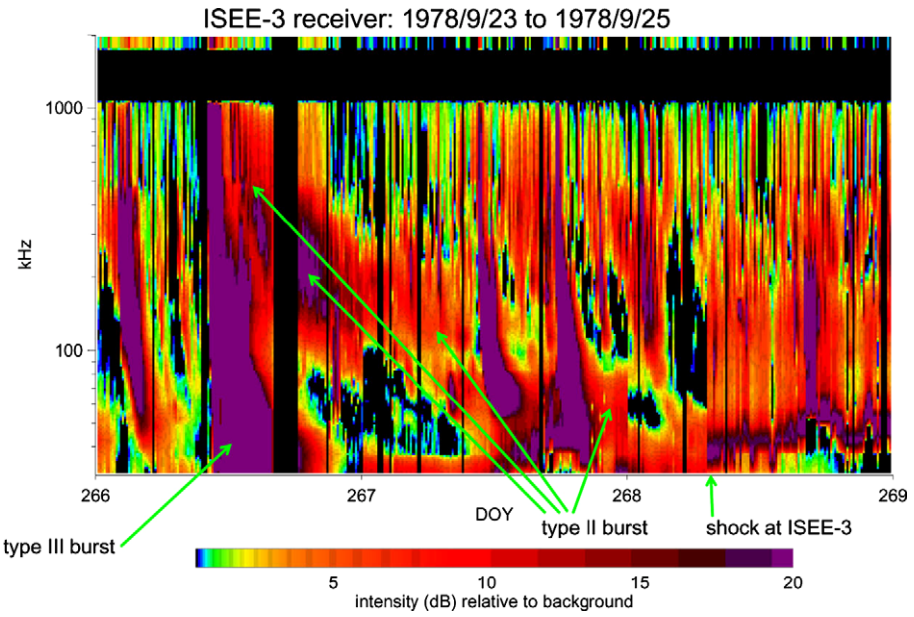

Fig. 4. Spectrogram as a function of time of the radio emission received at 1 AU. Color scale is given in decibels. (For interpretation of the references to color in this figure legend, the reader is referred to the web version of this paper.)

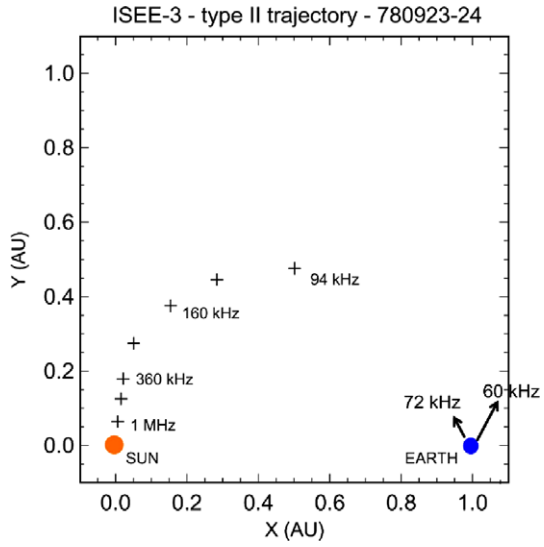

Fig. 5. Heliographic source location of the type II radio burst emissions. (See discussion in text.).

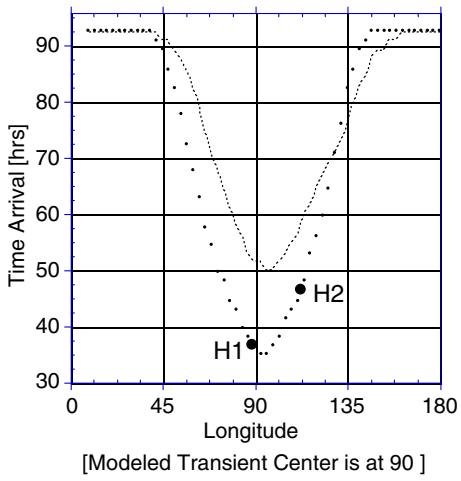

Fig. 6. H1, H2, and two 3D MHD modeled longitude dependence of the time of arrival at 1 AU of the shock.

momentum located at 18 solar radii, within a solid angle range of 24° × 24°. (The reason for the initial input distance is that the implementation of the model requires the presence of a supersonic plasma environment.) The first run (small dots in Fig. 6) corresponds to a ramped up momentum, which combines a ΔV of 400 km^{-1} during 3 h and a plasma density ten times higher than the one modeled for a steady background solar wind with a speed of 400 km^{-1}. This value is an approximation to the pre-shock solar wind speed observed at Helios 2 and in Earth's vicinity, and earlier at Helios 1; These parameters are justified because of the assumed source near central meridian (6°E, see Burlaga et al., 1981). A second run indicated by a separated-point line in Fig. 6, shows that the right time-of-arrival can be modeled with a higher input in momentum for the transient. In this case a $\Delta V = 800$ km^{-1} input for 12 h for the same condition of ten times the ratio of disturbance-density to background solar wind was employed.

A comparison of the time series of modeled parameters at 1 AU with those observed at Helios 1 (using simple ballistic propagation from its location at 0.95–1 AU) is made in Fig. 7. First we note that due to a lack of dense grid points, the sharp discontinuity at shock passage is missing. Further, Fig. 7 shows that the modeling qualitatively reproduces the time series for the observed number density (N). It mimics the enhancement of N several hours behind

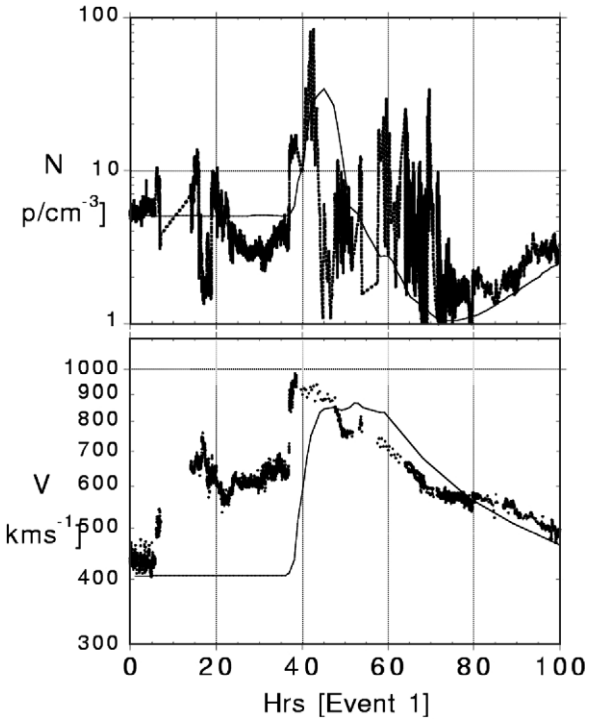

Fig. 7. The observed (H1) and modeled (smooth curve) time series for the number particle N, and plasma velocity V from the start time at Sun, Event 1.

the shock to values well above the compression limit of a factor of four (MHD R–H condition), as well as gives the later, overall long lasting reduction in the plasma density. The modeled speed (V) has a time profile that shows the overall observed velocity rise after shock passage, although it reaches maximum later, and is off by ~15%. The modeled V also shows a decrease similar to the observed, which is consistent with the expansion of the disturbance in space as it propagates away from the Sun. There is qualitative agreement also for the solar wind V and N at Helios 2 (not shown because of space limitations). The agreement does not extend to the observed magnetic field of the ejecta; this is expected, considering that the introduced disturbances did not contain a magnetic structure.

4. Conclusions

For a moderate and an intense SEP event we tried to identify a possible link between the shocks here studied and the gradual SEP coincident in the same time and location intervals. The identified link here is, in each case, the presence of a shock region that moves more than 300 km^{-1} faster than the solar wind stream being overtaken. We further explored the shock characteristics for the moderate SEP event of Jan 1978 and identified the presence of near strong shock conditions at one shock passage location. Further, we explored the time passage at each location and the fitting of the solar wind parameters with the 3D MHD model. The model showed that at its fastest location (Helios 1) the shock surface was 6° West from the nose (Fig. 6), and qualitatively reproduced the local observed high speed of the in-situ shock passage (Fig. 7). The slower speed at Helios 2 was located further away, approximately 30° East from the nose (Fig. 6). In the case of the September 1978 intense SEP event the remote sensing identifies a region of shock velocity far faster than any corotating solar wind stream (>1600 km^{-1}), which likely implies a much larger strong-shock-region that than on January 1978. These results are consistent with a correlation of the SEP event sizes to the extension of strong shock portion of the global shock surfaces. As proposed earlier (Sanahuja et al., 1981), we conclude that the nose of the shocks that are associated with SEP gradual events slow down less/little over the heliographic distances of interest ($\leqslant$1 AU). As proposed earlier (Sanahuja et al., 1981), we conclude that the nose regions of these shocks slow down less/little over the heliographic distances of interest ($\leqslant$1 AU).

We find agreement of the modeled time-of-arrival of the shock with observation, for a 24° × 24° localized disturbance at the Sun, under the assumption of an extreme (and abrupt?) momentum addition. In the case, of a perturbation that likely lasted 1 h at 18 solar radii, the modeled transient would indicate a momentum input, in 1 h, of at least 100 times the momentum of the background solar wind.

Acknowledgements

We acknowledge the COHO and OMNI data base for hourly and higher resolution averages of the IP parameters. This work is supported by NASA Living with a Star Grant NASW-02035, and NSF Space Weather Grant ATM-0208414.

References

Berdichevsky, D., Szabo, A., Lepping, R.P., Viñas, A.F., Mariani, F. Interplanetary fast shocks and associated drivers observed through the twenty-third solar minimum by wind over its first 2.5 years. J. Geophys. Res. 105 (27), 227–289, Errata in J. Geophys. Res., 106, 25,133, 2001, 2000.

Burlaga, L.F., Sittler, E., Mariani, F., Schwenn, R. Magnetic loop behind an interplanetary shock: Voyager, Helios, and IMP-8 observations. J. Geophys. Res. 86, 6673–6684 , 1981.

Cane, H.V. The evolution of interplanetary shocks. J. Geophys. Res. 90, 191–197, 1985.

Cane, H.V., Reames, D.V., von Rosenvinge, T.T. The role of interplanetary shocks in the longitude distribution of solar energetic particles. J. Geophys. Res. 93, 9555–9567, 1988.

Detman, T.R., Dryer, M., Yeh, T., Wu, S.T., McComas, D.J. A time dependent three dimensional MHD numerical study of interplanetary magnetic draping ground plasmoids in the solar wind. J. Geophys. Res. 96, 9531–9940, 1991.

Fainberg, J. Technique to determine location of radio sources from measurements taken on spinning spacecraft. NASA Tech. Memorandum 80598, 1979.

Fainberg, J., Hoang, S., Manning, R. Measurements of distributed polarized radio sources from spinning spacecraft; effect of a tilted axial antenna. ISEE-3 application and results. Astron. Astrophys. 153, 145–150, 1985.

Han, S.M., Wu, S.T., Dryer, M. A three dimensional, time dependent numerical modeling of supersonic, super Alvenic MHD flow. Comput. Fluids 16, 81–103, 1988.

Heras, Sanahuja, A.M.B., Domingo, V., Joselyn, J.A. Low-energy particle events generated by solar disappearing filaments Astron. Astrophys. 197, 297–305, 1988.

Kahler, S.W. The correlation between solar energetic particle peak intensities and speeds of coronal mass ejections: effects of ambient particle intensities and energy. J. Geophys. Res. 106, 20947–20955, 2001.

Knoll, R., Epstein, G., Hoang, S., Huntzinger, G., Steinberg, J.L., Fainberg, J., Grena, F., Mosier, S.R., Stone, R.G. The three dimensional radio mapping experiment (SBH) on ISEE-C. Trans. Geosci. Electron. GE-16, 199–204, 1978.

Reames, D.V., Barbier, L.M., Ng, C.K. The spatial distribution of particles accelerated by coronal mass ejection-driven shocks. ApJ 466, 473–486, 1996.

Reames, D.V., Kahler, S.W., Ng, C.K. Spatial and temporal invariance in the spectra of energetic particles in gradual solar events. ApJ 491, 414–420, 1997.

Reames, D.V. Particle acceleration at the Sun and in the heliosphere. Space Sci. Rev. 90, 413–491, 1999a.

Reames, D.V. Particle acceleration at CME-driven shock waves. In: Dingus, B.L., Kieda, D.B., Salamon, M.H. (Eds.), 26th International Cosmic Ray Conference, AIP Conf. Series 516, 289, 1999b.

Reames, D.V. SEPs: Space weather hazard in interplanetary space, in: Song, P., Singer, H.J. (Eds.), Space weather, Geophysical Monograph, vol. 125. American Geophysical Union, Wasington, DC, pp. 101–107, 2001.

Richardson, G.L., Wibberenz, J.G.G., Cane, H.V., The relationship between recurring cosmic ray depressions and corotating solar wind streams at $\leqslant$1 AU; IMP8 and Helios 1 and 2 anticoincidence guard rate observations, J. Geophys. Res. 101, 13483, 1996.

Sanahuja, B., Domingo, V., Wenzel, K.-P., Joselyn, J.A., Keppler, E. A large proton event associated with solar filament activity. Sol. Phys. 84, 321–337, 1981.

Turner, R. What we must know about solar particle events to reduce the risk to astronauts, in: Song, P., Singer, H.J., Siscoe, G.L. (Eds.), AGU Monograph on Space Weather, vol. 125, pp 101–107, 2001.

Wu, C-C., Fry, C.D., Berdichevsky, D.B., Dryer, M., Smith, Z., Detman, T. Predicting the arrival time of shock passages at Earth. Sol. Phys. 227, 371–386, 2005.

Please cite this article in press as: Berdichevsky, D.B. et al., Exploring the global shock scenario at multiple points between sun ..., J. Adv. Space Res. (2008), doi:10.1016/j.asr.2008.03.026